Sharing of mitotic pre-ribosomal particles between daughter cells.

Valentina Sirri, Nathalie Jourdan, Danièle Hernandez-Verdun, Pascal Roussel

© 2016. Published by The Company of Biologists Ltd | Journal of Cell Science (2016) 129, 1592-1604 doi:10.1242/jcs.180521

RESEARCH ARTICLE

Sharing of mitotic pre-ribosomal particles between daughter cells

Valentina Sirri[1], Nathalie Jourdan[2], Danièle Hernandez-Verdun[3] and Pascal Roussel[1,*]

ABSTRACT

Ribosome biogenesis is a fundamental multistep process initiated by the synthesis of 90S pre-ribosomal particles in the nucleoli of higher eukaryotes. Even though synthesis of ribosomes stops during mitosis while nucleoli disappear, mitotic pre-ribosomal particles persist as observed in pre-nucleolar bodies (PNBs) during telophase. To further understand the relationship between the nucleolus and the PNBs, the presence and the fate of the mitotic pre-ribosomal particles during cell division were investigated. We demonstrate that the recently synthesized 45S precursor ribosomal RNAs (pre-rRNAs) as well as the 32S and 30S pre-rRNAs are maintained during mitosis and associated with the chromosome periphery together with pre-rRNA processing factors. Maturation of the mitotic pre-ribosomal particles, as assessed by the stability of the mitotic pre-rRNAs, is transiently arrested during mitosis by a cyclin-dependent kinase (CDK)1-cyclin-B-dependent mechanism and can be restored by CDK inhibitor treatments. At the M–G1 transition, the resumption of mitotic pre-rRNA processing in PNBs does not induce the disappearance of PNBs; this only occurs when functional nucleoli reform. Strikingly, during their maturation process, mitotic pre-rRNAs localize in reforming nucleoli.

KEY WORDS: Nucleolus, PNB, Mitosis, Ribosomal RNA

INTRODUCTION

The synthesis of ribosomes is a highly complex multistep process requiring the RNA polymerases (Pol) I, Pol II and Pol III, and several hundred accessory factors in addition to the ribosomal proteins and ribosomal RNAs (rRNAs). In eukaryotes, ribosome biogenesis begins in the nucleolus with Pol-I-dependent transcription of a precursor ribosomal RNA (47S pre-rRNA in vertebrates) leading to the mature 18S, 5.8S and 28S rRNAs. Ribosomal and non-ribosomal proteins and small nucleolar ribonucleoproteins (RNPs) co-transcriptionally associate with 47S pre-rRNA and form 90S pre-ribosomal particles that then generate pre-40S and pre-60S ribosomal particles (Henras et al., 2008). These pre-ribosomal particles are further matured before being exported into the cytoplasm where the final processing steps generate mature ribosomal subunits. The progressive maturation of pre-ribosomal particles implies the stepwise assembly of ribosomal proteins and transient non-ribosomal processing factors, and occurs concomitantly with processing of the 47S pre-rRNA.

During mitosis, Pol-I-dependent transcription of ribosomal genes (rDNAs) is progressively repressed during prophase and maintained repressed in a cyclin-dependent kinase (CDK)1–cyclin-B-dependent manner until telophase (Sirri et al., 2000). The resumption of rDNA transcription when CDK1–cyclin B is inactivated constitutes the first step in the formation of the nucleolus as well as in restoring ribosome biogenesis at the exit from mitosis (Sirri et al., 2000, 2002). Research in ribosome biogenesis has unraveled the pathways of 47S pre-rRNA processing (Mullineux and Lafontaine, 2012) and revealed how this complex process involves several hundred pre-rRNA processing factors (Tafforeau et al., 2013). Considering the large number of pre-rRNA processing factors, little is yet known of the fate of the pre-rRNA processing machinery during mitosis while ribosome biogenesis is turned off and nucleoli are no longer maintained. However, during cell division, several pre-rRNA processing factors, such as fibrillarin, nucleolin, Nop52 (also known as RRP1) and NPM (also known as B23), are co-localized at the periphery of chromosomes from prophase to telophase and then in pre-nucleolar bodies (PNBs) until the early G1 phase (Dundr et al., 2000; Gautier et al., 1992; Hügle et al., 1985; Savino et al., 1999). As reported recently (Booth et al., 2014), the localization at the chromosome periphery depends on the protein Ki-67. In addition to proteins, small nucleolar RNAs involved in pre-rRNA processing such as U3, U8, and U14 (Dousset et al., 2000; Jiménez-García et al., 1994) are observed in PNBs. Furthermore, in addition to these non-ribosomal processing factors, pre-rRNAs (Boisvert et al., 2007; Carron et al., 2012; DiMario, 2004; Dundr et al., 2000; Fan and Penman, 1971; Phillips, 1972) as well as ribosomal proteins (Carron et al., 2012; Gassmann et al., 2004; Hügle et al., 1985; Ohta et al., 2010) are observed on the chromosome periphery and in PNBs. It was also proposed that the association of pre-rRNAs with proteins in pre-rRNP complexes is maintained during mitosis (Piñol-Roma, 1999), and recently pre-ribosomal particles were reported in PNBs (Carron et al., 2012).

Despite extensive studies on nucleologenesis, it remains unclear how pre-rRNA processing is restored, and what role is played by PNBs. However time-lapse microscopy analyses have clearly shown the relationship between PNBs and reforming nucleoli (Dundr et al., 2000; Savino et al., 1999). Based on their ultrastructure and composition, PNBs were initially thought to be a step prior to the formation of nucleoli. Because PNBs differ in their components and lifetimes, it was proposed that different types of PNBs exist that are targeted to reforming nucleoli with different kinetics (Savino et al., 1999, 2001; Westendorf et al., 1998). Beyond the dynamics of postmitotic formation of nucleoli, PNBs themselves are highly dynamic structures (Dundr et al., 2000; Muro et al., 2010). Recently, PNBs were proposed to be the sites where maturation of the pre-rRNAs transiting through mitosis is restored in telophase. PNBs would be autonomous extra-nucleolar ribosome maturation sites whose disassembly in G1 phase is governed by processing and release of their pre-ribosome content (Carron et al., 2012).

To further understand the relationship between PNBs and nucleoli, we examined the fate of mitotic pre-ribosomal particles

[1]Université Paris Diderot, Unit of Functional and Adaptive Biology, UMR 8251 CNRS, 4 rue Marie-Andrée Lagroua Weill-Hallé, Paris F-75205, France. [2]UPMC Université Paris 06, Institut de Biologie Paris Seine, UMR 8256 CNRS, 9 quai St Bernard, Paris F-75252, France. [3]Université Paris Diderot, Institut Jacques Monod, UMR 7592 CNRS, 15 rue Hélène Brion, Paris F-75205, France.

*Author for correspondence (p.roussel@univ-paris-diderot.fr)

Received 16 September 2015; Accepted 20 February 2016

Journal of Cell Science

Journal of Cell Science (2016) 129, 1592-1604 doi:10.1242/jcs.180521

by mitotic pre-rRNAs (m-pre-rRNAs), during cell division. Recently synthesized 45S pre-rRNAs, as well as 32S and 30S pre-rRNAs are maintained when nucleoli disappear. They associate with the chromosome periphery together with pre-rRNA processing factors. Maturation of mitotic pre-ribosomal particles is transiently arrested during mitosis and can be restored by CDK inhibitor treatments. At M–G1 transition, processing of m-pre-rRNAs does not induce dissolution of PNBs that depends on the reformation of functional nucleoli. During their maturation process, m-pre-rRNAs localize in reforming nucleoli and therefore might participate in the reformation of nucleoli in early G1 cells.

RESULTS

In human cells, rDNA transcription gives rise to 47S pre-rRNA initially cleaved at both ends to generate 45S pre-rRNA, then processed by two alternative pathways to generate mature 18S, 5.8S and 28S rRNAs (Fig. S1). During mitosis, rDNA transcription is progressively repressed during prophase and restored in telophase (Fig. S2) but pre-rRNAs – thereafter designated m-pre-rRNAs – are maintained. Here, we have globally followed the fate of metabolically labeled m-pre-rRNAs during and at exit from mitosis. For this purpose, 5-ethynyl uridine (EU) was used as modified uridine because, in contrast to 5-fluorouridine (FU) (Wilkinson et al., 1975), it does not alter pre-rRNA processing.

The last pre-rRNAs synthesized localize at the chromosome periphery

To assess synthesis of m-pre-rRNAs, double metabolic labeling of RNAs in asynchronous HeLa cells was performed. To discriminate between the earlier- and later-synthesized RNAs, EU incorporation was allowed for 3 h, whereas FU incorporation was only allowed for the last 30 min before cell fixation. The localization of EU- and FU-labeled RNAs was compared with that of the nucleolar marker fibrillarin (Fig. 1A–F). In interphase cells, EU- and FU-labeled RNAs were observed mainly in nucleoli identified by fibrillarin (Fig. 1A) as well as in prophase cells, whereas rDNA transcription was progressively repressed (Fig. 1B). The EU-labeled RNAs were localized at the chromosome periphery in all transcriptionally inactive mitotic stages similarly to fibrillarin (Fig. 1C–F). This observation demonstrates that RNAs synthesized before transcription repression are maintained during mitosis and localize at the chromosome periphery. Because synthesis of such metabolically labeled RNAs is largely prevented by inhibition of rDNA transcription [through addition of the transcription inhibitor actinomycin D (AMD)] (Fig. 2A, +AMD), these mitotic RNAs are mostly m-pre-rRNAs. Interestingly, FU-labeled m-pre-rRNAs co-localized with fibrillarin in the early mitotic stages as observed in prometaphase (Fig. 1C) and in some metaphase cells (Fig. 1D,E) but not in later mitotic stages as illustrated for late anaphase (Fig. 1F). As (1) FU incorporation lasted only 30 min, (2) rDNA transcription is repressed in prophase and (3) the average time needed for HeLa cells to progress from the end of prophase (nuclear envelope breakdown) to metaphase (full chromosome alignment) is 20 min (Chen et al., 2008; Toyoda and Yanagida, 2006), the absence of FU-labeled m-pre-rRNAs was expected in later mitotic stages and showed the specificity of the *in situ* detections of FU- and EU-labeled RNAs. More interestingly, the presence of FU-labeled m-pre-rRNAs in early mitotic stages demonstrated that the most recently synthesized pre-rRNAs persist during mitosis and localize at the chromosome periphery.

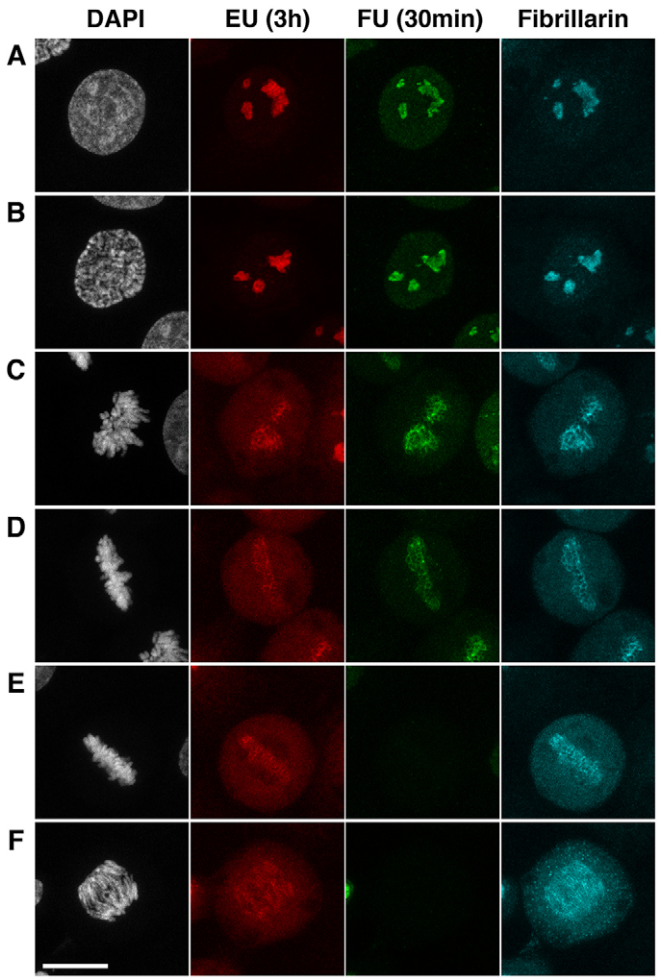

Fig. 1. Last pre-rRNAs synthesized localize at the chromosome periphery. HeLa cells were cultured in medium containing EU for 3 h, FU being added for the last 30 min. EU and FU incorporations were revealed and fibrillarin detected. The period of the cell cycle is identified by DAPI staining: interphase (A), prophase (B), prometaphase (C), metaphase (D and E) and late anaphase (F). Scale bar: 10 µm.

m-pre-rRNAs determine the localization of nucleolar proteins at the chromosome periphery

To assess the relationship between m-pre-rRNAs and the localization of nucleolar proteins during mitosis, a double metabolic labeling of RNAs was performed on asynchronous HeLa cells (Fig. 2A). EU incorporation lasted 3 h before cell fixation whereas FU incorporation was limited to the last 1 h, a period sufficient to ensure FU labeling of m-pre-rRNAs in all metaphase cells. The cells were treated or not with AMD during the last 1 h of culture to specifically inhibit pre-rRNA synthesis. EU and FU incorporations were detected in metaphase cells and the localization of EU- and FU-labeled m-pre-rRNAs compared with that of fibrillarin. In control cells (Fig. 2A, −AMD), EU- and FU-labeled m-pre-rRNAs co-localized with fibrillarin around the chromosomes. When pre-rRNA synthesis was inhibited (Fig. 2A, +AMD), both the FU- and EU-labeled m-pre-rRNAs were greatly reduced. The residual FU-labeling observed after AMD treatment was most probably due to detection of pre-rRNAs synthesized during the 10 min before effective inhibition of rDNA transcription (Popov et al., 2013). More interestingly, the large decrease of these m-pre-rRNAs induced delocalization of fibrillarin from the

Journal of Cell Science (2016) 129, 1592-1604 doi:10.1242/jcs.180521

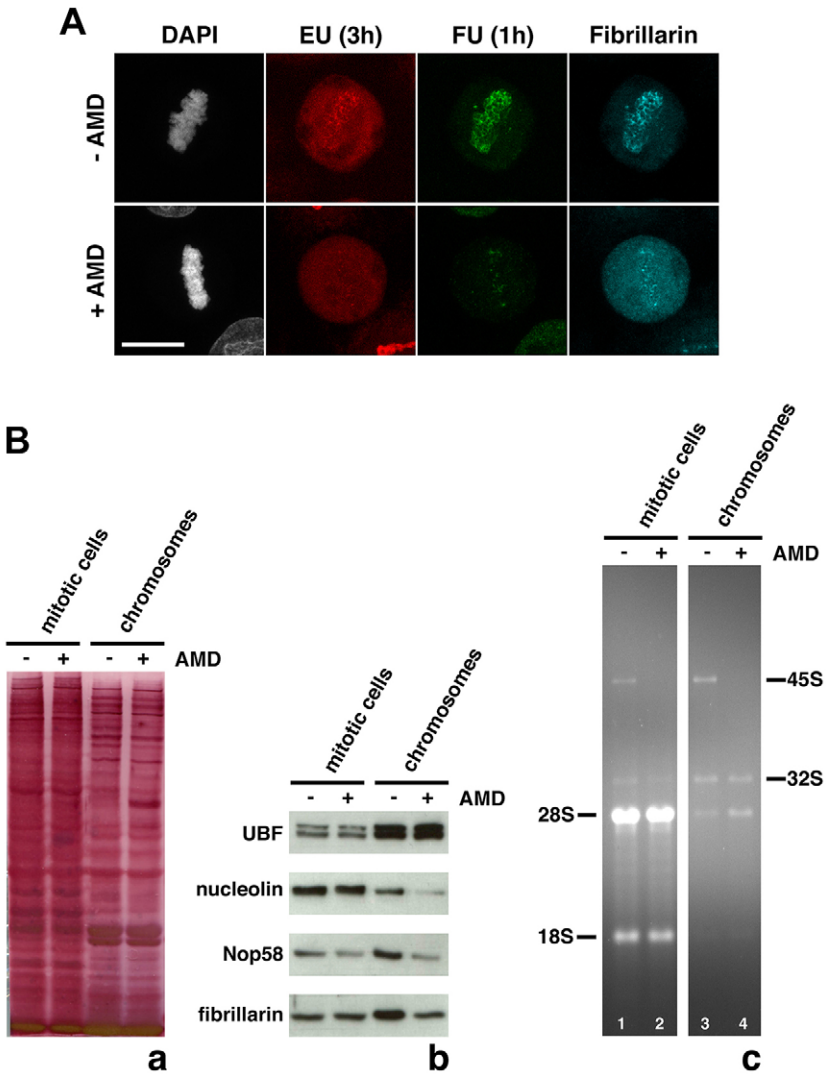

Fig. 2. m-pre-rRNAs determine the localization of nucleolar proteins at the chromosome periphery. (A) HeLa cells were cultured in medium containing EU for 3 h and FU was added for the last hour in the absence (–) or presence (+) of AMD. EU and FU incorporations were revealed and fibrillarin detected in metaphase cells. Scale bar: 10 µm. (B) Protein and RNA extracts from whole (mitotic) cells and chromosomes were prepared from prometaphase HeLa cells, harvested in the presence (+) or absence (–) of AMD. Protein extracts were analyzed by total protein staining (Ba) and immunoblotting (Bb) using anti-UBF, anti-nucleolin, anti-Nop58 and anti-fibrillarin antibodies. RNAs were resolved on gels and stained with ethidium bromide (EtBr) (Bc).

chromosome periphery to the cytoplasm (Fig. 2A, +AMD). This observation was reinforced by results obtained after siRNA depletion of nucleolin, known to play an important role in pre-rRNA synthesis (Fig. S3). As assessed by FU incorporation in nucleoli of interphase cells, rDNA transcription largely decreased in nucleolin-depleted HeLa cells and consequently, also the amount of m-pre-rRNAs present at the chromosome periphery during mitosis. The decrease of m-pre-rRNAs also induced delocalization of fibrillarin from the chromosome periphery to the cytoplasm.

These results brought into question the relationship between the presence of m-pre-rRNAs and the localization of nucleolar proteins at the chromosome periphery. To further analyze the influence of m-pre-rRNAs on protein–chromosome association, western blots were performed on extracts prepared from HeLa cells accumulated in prometaphase for 4 h in the presence or absence of AMD, and from their isolated chromosomes (Fig. 2Ba,b). Nucleolar proteins involved in pre-rRNA processing and localized at the chromosome periphery, namely fibrillarin, nucleolin and Nop58, were analyzed and compared with the transcription factor UBF. Interestingly, the amounts of nucleolin, Nop58 and fibrillarin were lower in chromosome extracts prepared from AMD-treated cells compared with control cells. Conversely, UBF seemed enriched in chromosome extracts regardless of AMD treatment. Thus, the perichromosomal localization of these pre-rRNA processing factors depends on the presence of m-pre-rRNAs and most probably on direct and/or indirect interaction with m-pre-rRNAs.

Total RNAs were also prepared from HeLa prometaphase cells treated or not with AMD and from chromosomes (Fig. 2Bc) to further analyze the effects of AMD treatment on the presence of m-pre-rRNAs. Ethidium bromide (EtBr) staining of RNAs after electrophoretic separation showed first that the 45S and 32S pre-rRNAs were enriched in RNA extracts from chromosomes isolated from control cells (Fig. 2Bc, lane 3) in contrast to mature 28S and 18S rRNAs (Fig. 2Bc, lanes 1, 3), showing that 45S and 32S pre-rRNAs co-purified with chromosomes. The EtBr staining showed also that the 45S pre-rRNA disappeared after AMD-induced inhibition of pre-rRNA synthesis, whereas the 32S pre-rRNA only decreased slightly (Fig. 2Bc, lanes 1–4). The fact that m-pre-rRNAs present at the chromosome periphery not only correspond to pre-rRNAs synthesized during AMD treatment most probably accounts for the presence of residual amounts of pre-rRNA processing factors at the chromosome periphery of AMD-treated cells (Fig. 2Bb).

Identification of m-pre-rRNAs associated with chromosomes and their fate at exit from mitosis

The identification of m-pre-rRNAs associated with chromosomes was performed by northern blot. Use of a 5.8S+ probe allowed

Journal of Cell Science (2016) 129, 1592-1604 doi:10.1242/jcs.180521

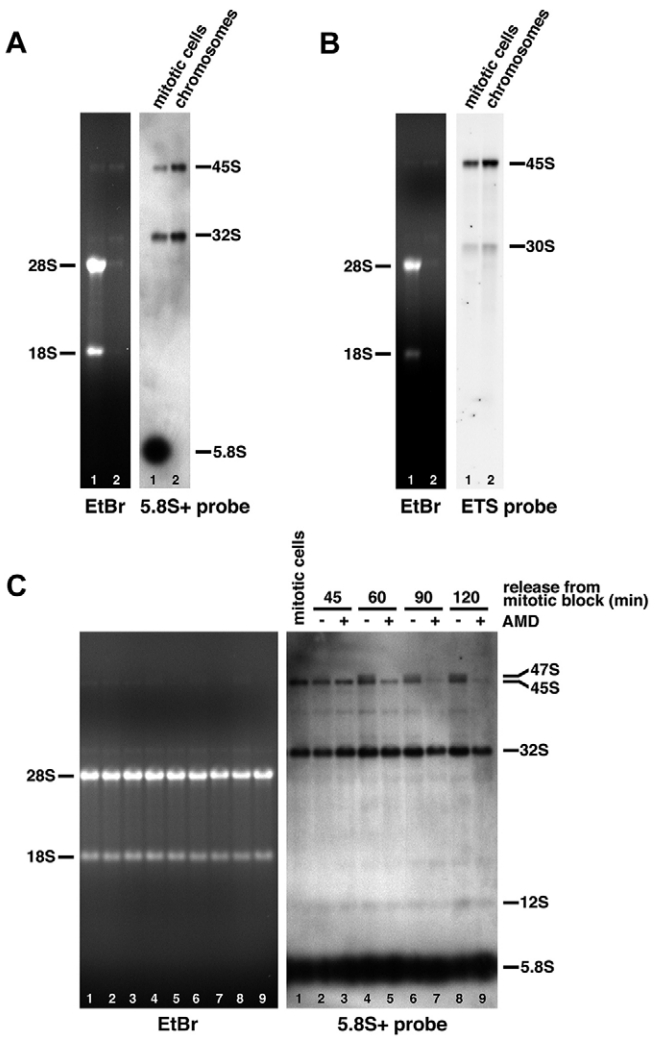

Fig. 3. Identification of m-pre-rRNAs and their fate at exit of mitosis. (A,B) RNAs extracted from colcemid-blocked prometaphase HeLa cells (mitotic cells) and from purified chromosomes were resolved on gels (EtBr), blotted and hybridized with the 5.8S+ (A) and ETS (B) probes. (C) Nocodazole-blocked prometaphase HeLa cells were released into nocodazole-free medium containing (+) or not (–) AMD. RNAs were prepared from cells at 45, 60, 90 and 120 min, analyzed in a gel (EtBr), blotted and hybridized with the 5.8S+ probe.

detection of 47S, 46S, 45S, 43S, 41S, 32S and 12S pre-rRNAs and mature 5.8S rRNA (Fig. 3A; Fig. S1), whereas an ETS probe allowed detection of 47S, 46S, 45S and 30S pre-rRNAs (Fig. 3B; Fig. S1) and an 18S probe allowed detection of 47S, 46S, 45S, 43S, 41S, 30S, 26S, 21S and 18S-E pre-rRNAs and mature 18S rRNA (Figs S1, S4). The identification of 45S and 32S pre-rRNAs as being m-pre-rRNAs was confirmed using the 5.8S+ probe (Fig. 3A). As observed for mature 28S and 18S rRNAs, mature 5.8S rRNA was visible in mitotic cells but not associated with chromosomes (Fig. 3A, lanes 1, 2). In addition, the 5.8S+ probe did not reveal the presence of 47S, 46S, 43S, 41S and 12S pre-rRNAs in mitotic cells or in chromosome extracts. The use of the ETS probe (Fig. 3B) confirmed the absence of 47S and 46S pre-rRNAs and the presence of 45S pre-rRNA and revealed the association of 30S pre-rRNAs with chromosomes. Noticeably, comparing the level of 45S pre-rRNA with that of 32S pre-rRNA (Fig. 3A) or of 30S pre-rRNA (Fig. 3B) showed that the amount of 30S pre-rRNA is low compared with that of 45S and 32S pre-rRNA. The use of the 18S probe (Fig. S4) confirmed these results and did not reveal additional pre-rRNA quantitatively associated with chromosomes.

To assess the fate of the major m-pre-rRNAs, namely 45S and 32S pre-rRNAs, when cells exit from mitosis, prometaphase-arrested HeLa cells were released from the mitotic block in the absence or presence of AMD and total RNAs analyzed by northern blot using the 5.8S+ probe (Fig. 3C). This analysis showed that the cells progressed and exited from mitosis as demonstrated by the restoration of 47S pre-rRNA synthesis (Fig. 3C, lanes 1, 2, 4, 6, 8). When pre-rRNA synthesis was prevented by AMD, 45S pre-rRNA (Fig. 3C, lane 1) progressively disappeared (Fig. 3C, lanes 1, 3, 5, 7, 9). Interestingly, 32S pre-rRNA was still clearly observed after 120 min (Fig. 3C, lanes 1, 3, 5, 7, 9), showing that 32S pre-rRNA possesses a longer half-life than 45S pre-rRNA.

CDK inhibitors restore processing of m-pre-rRNAs

To investigate the possible effects of the CDK inhibitors roscovitine and indirubin-3′-monoxime on m-pre-rRNAs, prometaphase HeLa cells were first treated for 2 h with either AMD or one of the CDK inhibitors, or both AMD and a CDK inhibitor. The simultaneous use of AMD and CDK inhibitors allowed discrimination between m-pre-rRNAs and neosynthesized pre-rRNAs.

Total RNAs were analyzed by RT-qPCR quantification (Fig. 4Aa–c; Fig. S1) using primers ETS1 and ETS2 to quantify unprocessed 47S pre-rRNA, ETS3 and ETS4 to quantify 47S–30S pre-rRNAs, i.e. 47S, 46S, 45S and 30S pre-rRNAs, and 5.8S1 and 5.8S2 to quantify 47S–12S pre-rRNAs, i.e. 47S, 46S, 45S, 43S, 41S, 32S and 12S pre-rRNAs. The quantification of the 47S pre-rRNA showed that both roscovitine and indirubin-3′-monoxime induce resumption of rDNA transcription. Indeed, the amount of 47S pre-rRNA dramatically increased after CDK inhibitor treatments (Fig. 4Aa; ROSC and INDI) whereas no increase was observed using AMD or AMD together with one of the CDK inhibitors (Fig. 4Aa; AMD, AMD/ROSC and AMD/INDI). Global quantification of 47S–30S pre-rRNAs confirmed this observation (Fig. 4Ab; ROSC and INDI). Because in the absence of neosynthesized pre-rRNAs the primers ETS3 and ETS4 allow specific quantification of 45S and 30S pre-rRNAs, this also showed that the amount of 45S and 30S pre-rRNAs present in mitotic cells rapidly decreased after CDK inhibitor treatments (Fig. 4Ab, AMD, AMD/ROSC and AMD/INDI) and suggested that CDK inhibitors can induce degradation or processing of m-pre-rRNAs. Noticeably, the quantification of 47S–12S pre-rRNAs (Fig. 4Ac) was not in favor of random degradation but of progressive processing of the m-pre-rRNAs. Indeed, the large decrease observed for global quantification of 47S–30S pre-rRNAs after CDK inhibitor treatments (Fig. 4Ab, compare AMD with AMD/ROSC and AMD/INDI) was not observed for quantification of 47S–12S pre-rRNAs (Fig. 4Ac, compare AMD with AMD/ROSC and AMD/INDI).

Total RNAs were also analyzed by northern blot with the 5.8S+ probe (Fig. S1). This confirmed that both CDK inhibitor treatments induced the resumption of rDNA transcription as assessed by the presence of 47S pre-rRNA (Fig. 4B, ROSC and INDI) and a large decrease of 45S pre-rRNA clearly visible when rDNA transcription was simultaneously inhibited (Fig. 4B, AMD/ROSC and AMD/INDI). Quantification of the northern blot showed that the decrease of 45S pre-rRNA (Fig. 4Ca) occurred simultaneously with the increase of 32S pre-rRNA (Fig. 4Cb) and thus suggested that 45S pre-rRNA was most probably processed and not degraded. This suggested also that the processing of 45S pre-rRNA occurs much more rapidly than that of 32S pre-rRNA. The slow processing of

Journal of Cell Science (2016) 129, 1592-1604 doi:10.1242/jcs.180521

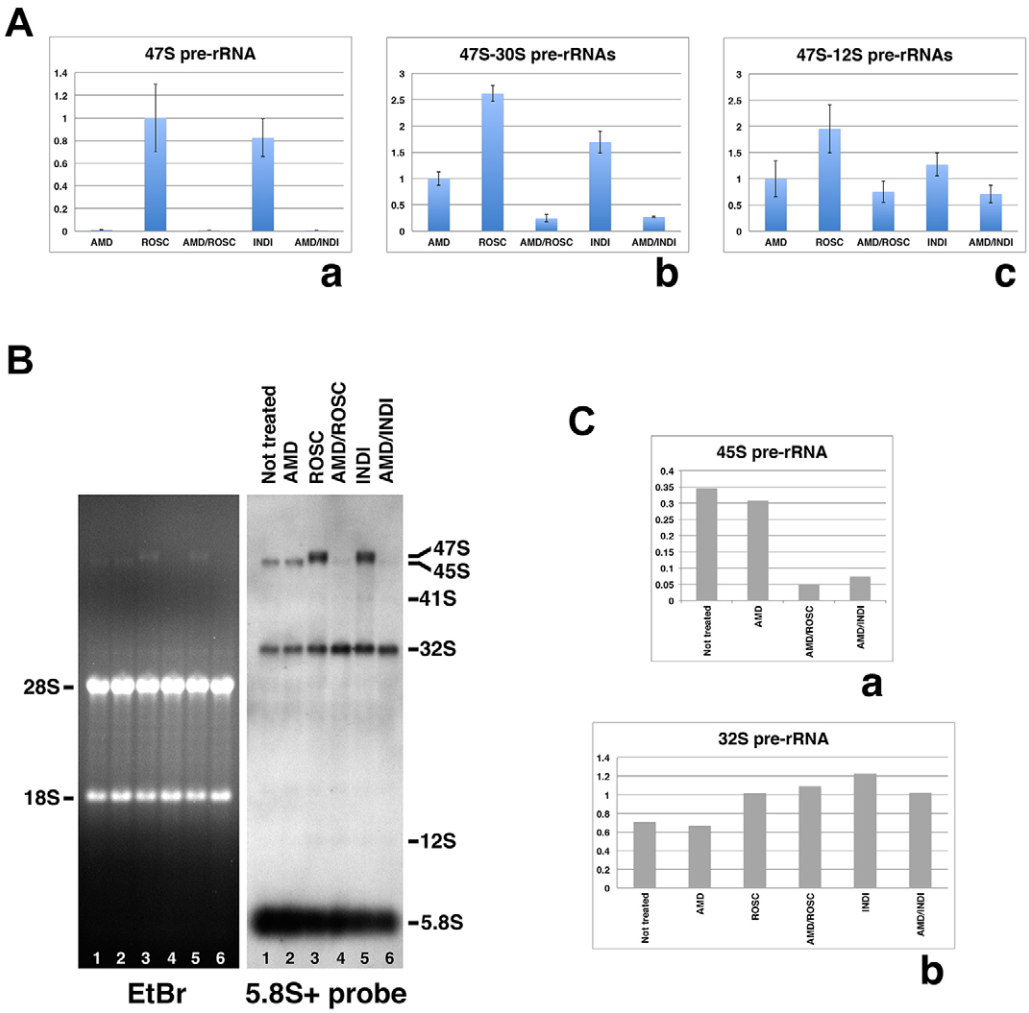

Fig. 4. CDK inhibitors restore processing of m-pre-rRNAs. (A–C) Colcemid-arrested prometaphase HeLa cells were not treated (Not treated) or treated in the presence of colcemid with AMD (AMD), roscovitine (ROSC), both AMD and roscovitine (AMD/ROSC), indirubin-3′-monoxime (INDI) or with both AMD and indirubin-3′-monoxime (AMD/INDI) for 2 h. (A) RT-qPCR analyses using primers ETS1 and ETS2 to quantify 47S pre-rRNA (Aa), primers ETS3 and ETS4 to quantify 47S–30S pre-rRNAs (Ab), and primers 5.8S1 and 5.8S2 to quantify 47S–12S pre-rRNAs (Ac) from three independent experiments. Error bars represent mean±s.d. (B) Northern blot analysis using the 5.8S+ probe. (C) Quantifications (expressed in arbitrary units) of 45S (Ca) and 32S (Cb) pre-rRNAs revealed in B.

32S pre-rRNA most probably explains the results obtained for quantifications of 47S–30S and 47S–12S pre-rRNAs after CDK inhibitor treatments (Fig. 4Ab,c).

To further understand the processing of m-pre-rRNAs and to compare the effects of roscovitine on the processing of neosynthesized pre-rRNAs with those of indirubin-3′-monoxime, northern blot analyses were performed on extracts prepared from mitotic cells treated as above for 2 or 6 h using the 5.8S+ (Fig. 5A) and ETS (Fig. 5C) probes. The results obtained by simultaneously using the CDK inhibitors and AMD confirmed that both CDK inhibitors most probably trigger processing of m-pre-rRNAs (Fig. 5A–D). Similarly to what was seen in asynchronous cells (Fig. 5A, lanes 8, 9), mitotic 32S pre-rRNA slowly decreased and was still observed after 6 h of CDK inhibitor treatments (Fig. 5A,B). Even if degradation cannot be completely ruled out, this argues in favor of processing of m-pre-rRNAs. Interestingly, roscovitine and indirubin-3′-monoxime differently affect processing of neosynthesized 47S pre-rRNA. Indeed, as we reported previously (Sirri et al., 2000), roscovitine led to the accumulation of unprocessed neosynthesized pre-rRNAs (Fig. 5A, lanes 2, 3, 8; Fig. 5C, lanes 2, 6). This processing defect results also in low levels of 32S, 30S and 12S pre-rRNAs (Fig. 5A–D). Conversely, indirubin-3′-monoxime induced both rDNA transcription and processing of transcripts as suggested when comparing the patterns obtained from extracts prepared from prometaphase cells treated with indirubin-3′-monoxime for 6 h and from untreated asynchronous cells and their quantifications (Fig. 5A–D). The processing of transcripts in mitotic cells treated with indirubin-3′-monoxime was most probably close to that occurring in interphase cells. Indeed, the percentage of 47S–45S pre-rRNAs and of either 32S and 12S pre-rRNAs (Fig. 5Ea), or 30S pre-rRNA (Fig. 5Eb) were similar in indirubin-3′-monoxime-treated prometaphase cells (Fig. 5Ea,b, INDI) and in untreated asynchronous cells (Fig. 5Ea,b, Async), contrary to what was observed in roscovitine-treated prometaphase cells (Fig. 5Ea,b, ROSC).

The CDK inhibitor indirubin-3′-monoxime induces relocation of m-pre-rRNAs in nucleoli

The fact that indirubin-3′-monoxime induced both rDNA transcription and processing of transcripts (Fig. 5A–E) that normally occur in nucleoli prompted us to verify the formation of nucleoli in indirubin-3′-monoxime-treated prometaphase cells. For

Journal of Cell Science (2016) 129, 1592-1604 doi:10.1242/jcs.180521

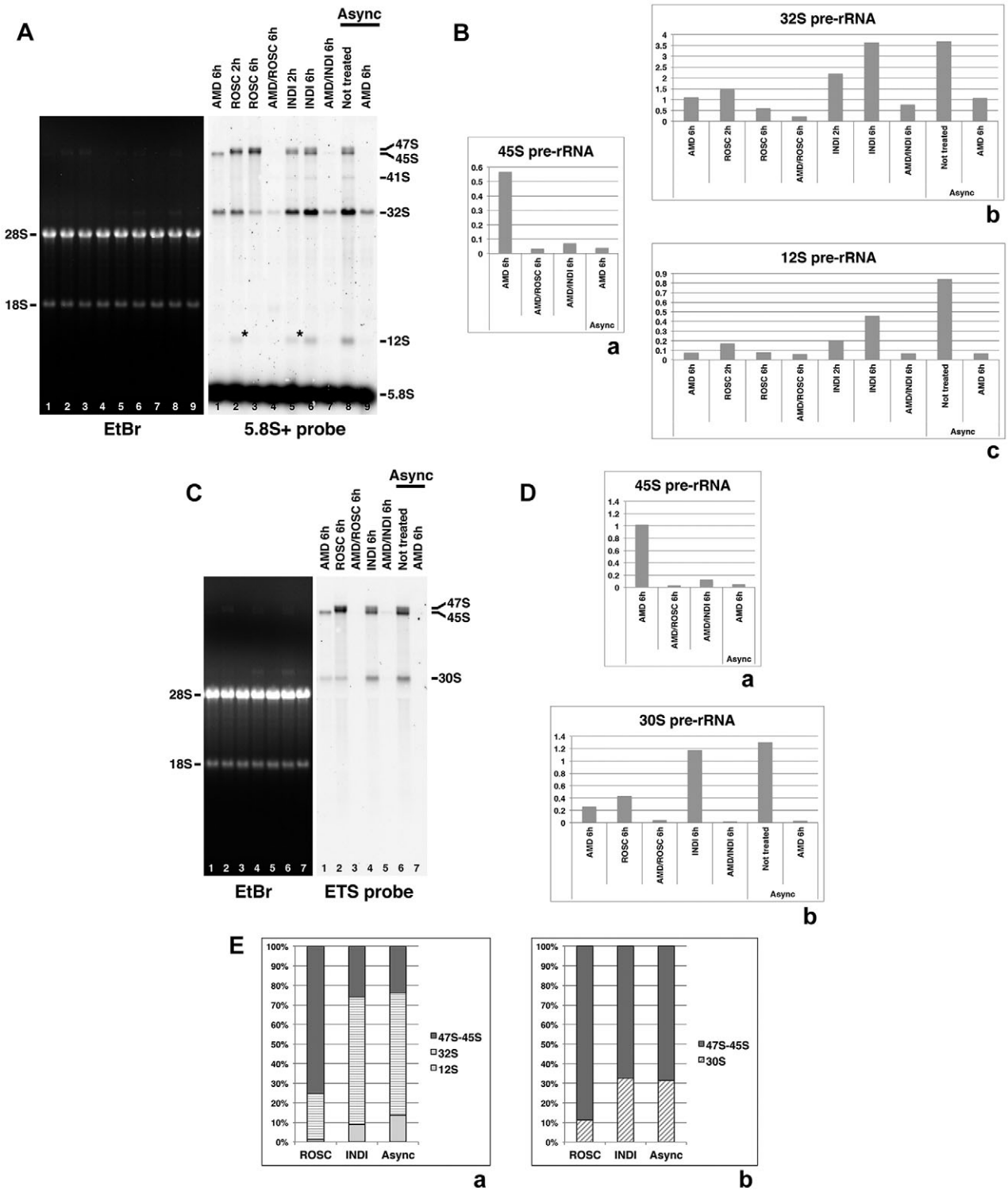

Fig. 5. CDK inhibitors restore processing of m-pre-rRNAs and differently affect processing of neosynthesized pre-rRNAs. (A–E) RNAs prepared from prometaphase HeLa cells treated as in Fig. 4 for 2 or 6 h, and from asynchronous HeLa cells (Async) treated or not with AMD for 6 h were separated in gels (EtBr), blotted and hybridized with the 5.8S+ probe (A) or the ETS probe (C). (B) Quantifications (expressed in arbitrary units) of 45S (Ba), 32S (Bb) and 12S (Bc) pre-rRNAs revealed in A. (D) Quantifications (expressed in arbitrary units) of 45S (Da) and 30S (Db) pre-rRNAs revealed in C. (E) Quantifications of 47S–45S, 32S and 12S pre-rRNAs revealed in A (Ea) and of 47S–45S and 30S pre-rRNAs revealed in C (Eb) for mitotic cells treated with roscovitine (ROSC) or indirubin-3′-monoxime (INDI) and untreated asynchronous cells (Async). Quantifications are expressed as a percentage of total hybridization signal.

this, the location of the nucleolar markers Nop52 and fibrillarin was analyzed in colcemid-arrested prometaphase Nop52–GFP HeLa cells treated with roscovitine (Fig. 6Aa), indirubin-3′-monoxime (Fig. 6Ab), both AMD and roscovitine (Fig. 6Ac) or with both AMD and indirubin-3′-monoxime (Fig. 6Ad) for 6 h. As already reported (Sirri et al., 2002), roscovitine treatment did not induce

Journal of Cell Science

Journal of Cell Science (2016) 129, 1592-1604 doi:10.1242/jcs.180521

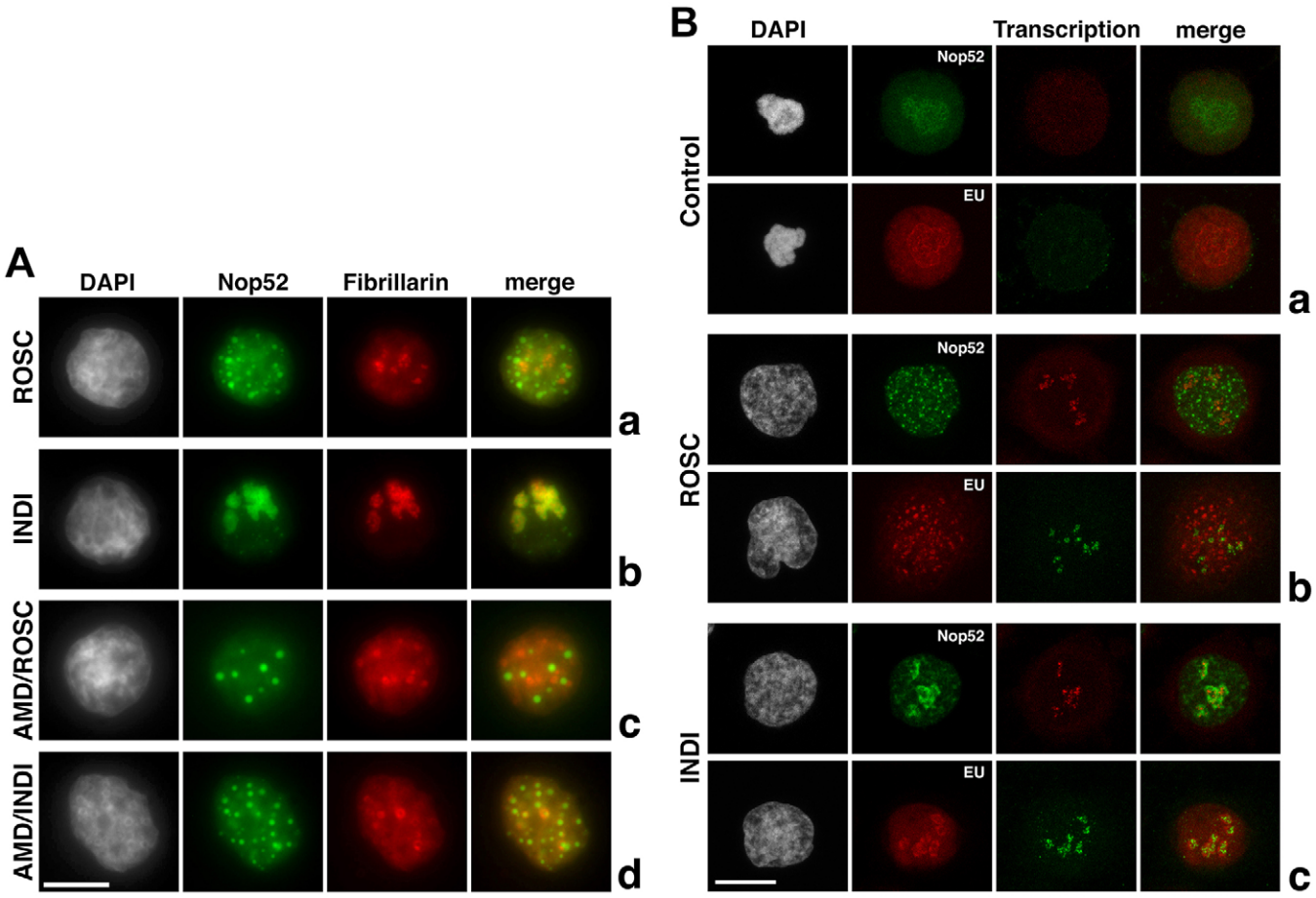

Fig. 6. The CDK inhibitor indirubin-3′-monoxime induces relocation of m-pre-rRNAs in nucleoli. (A) Colcemid-arrested prometaphase Nop52–GFP HeLa cells were treated in the presence of colcemid with roscovitine (Aa), indirubin-3′-monoxime (Ab), both AMD and roscovitine (Ac) or both AMD and indirubin-3′-monoxime (Ad) for 6 h and processed to observe Nop52 and fibrillarin. (B) Nop52–GFP and metabolically EU-labeled nocodazole-arrested prometaphase HeLa cells were untreated (Ba), treated with roscovitine (Bb) or with indirubin-3′-monoxime (Bc) for 2 h in the presence of nocodazole. Nop52–GFP HeLa cells were processed for Nop52 visualization and *in situ* detection of rDNA transcription. Metabolically EU-labeled HeLa cells were processed to reveal EU incorporation and to perform *in situ* detection of rDNA transcription. Scale bars: 10 µm.

formation of nucleoli and Nop52 localized in dots far from fibrillarin in roscovitine-treated cells (Fig. 6Aa). Conversely, formation of nucleoli was observed in indirubin-3′-monoxime-treated cells (Fig. 6Ab) as assessed by the gathering of both nucleolar markers in the same sites (Fig. 6Ab, merge). Noticeably, no formation of nucleoli was detected in cells treated with both AMD and CDK inhibitors (Fig. 6Ac,d), i.e. in conditions where rDNA transcription was impaired but not processing of m-pre-rRNAs (Fig. 5A–D), and Nop52-containing dots were observed.

Because CDK inhibitors exhibited different effects on nucleologenesis, we were intrigued by the fate of m-pre-rRNAs in roscovitine- or indirubin-3′-monoxime-treated mitotic cells. For this, Nop52–GFP expressing and metabolically EU-labeled prometaphase HeLa cells were either untreated (Fig. 6Ba) or treated with roscovitine (Fig. 6Bb) or indirubin-3′-monoxime (Fig. 6Bc) for 2 h. EU-labeled prometaphase cells were washed and treated with CDK inhibitors in an EU-free medium containing nocodazole so as to prevent EU uptake and therefore limit the synthesis of new EU-labeled pre-rRNAs, whereas the CDK inhibitor treatments triggered resumption of rDNA transcription. The cells were processed to visualize Nop52 (Fig. 6B, Nop52) or to reveal EU-labeled m-pre-rRNAs (Fig. 6B, EU) and to carry out *in situ* detection of rDNA transcription (Fig. 6B, Transcription). As expected (Sirri et al., 2002), Nop52 localized at the chromosome periphery in control cells (Fig. 6Ba, Nop52) and in small dots in roscovitine-treated cells (Fig. 6Bb, Nop52). The fact that Nop52-containing small dots were observed far from the sites of resumption of rDNA transcription (Fig. 6Bb, merge) confirmed that roscovitine impairs nucleologenesis. Similarly to Nop52 distribution, EU-labeled m-pre-rRNAs were detected at the chromosome periphery in control cells (Fig. 6Ba, EU) and as small dots in roscovitine-treated cells far from the sites of rDNA transcription (Fig. 6Bb, EU). In contrast to roscovitine, indirubin-3′-monoxime treatment induced the formation of nucleoli (Fig. 6Bc, Nop52) as argued by the gathering of Nop52 close to the sites of resumption of Pol I activity. Strikingly, EU-labeled RNAs were then observed in reformed nucleoli (Fig. 6Bc, EU). It should be noted that even if CDK inhibitor treatments were performed in an EU-free medium, we could not exclude the possibility that neosynthesized EU-labeled pre-rRNAs were also detected. However, because in roscovitine-treated cells, EU labeling was not or only weakly detected in the sites of resumption of rDNA transcription (Fig. 6Bb), neosynthesized EU-labeled pre-rRNAs were most probably negligible and therefore the EU-labeled RNAs observed in reformed nucleoli of indirubin-3′-monoxime-treated cells mainly corresponded to EU-labeled m-pre-rRNAs.

Journal of Cell Science (2016) 129, 1592-1604 doi:10.1242/jcs.180521

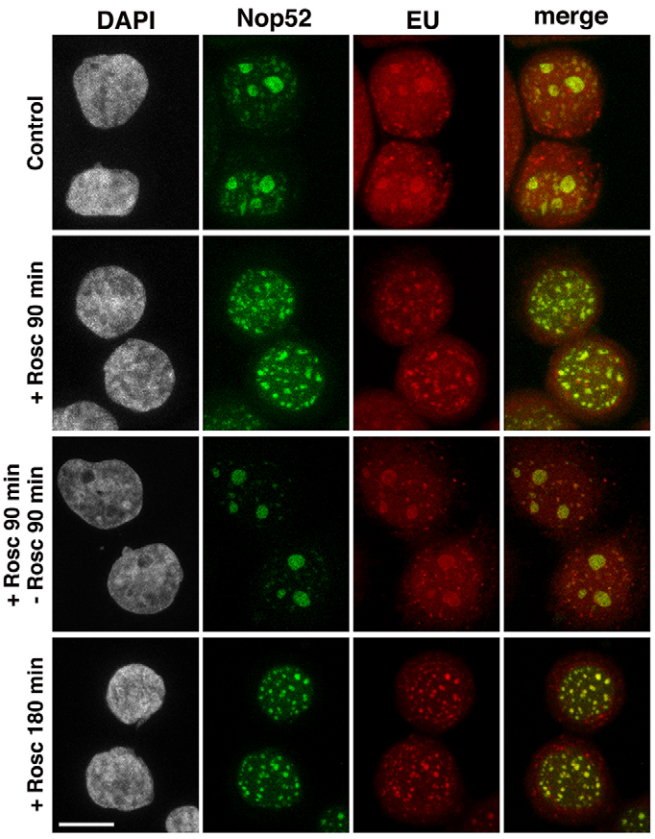

Fig. 7. m-pre-rRNAs relocate from PNBs to nucleoli at M–G1 transition. Nocodazole-arrested prometaphase Nop52–GFP HeLa cells accumulated in the presence of EU were washed and released into nocodazole-free medium containing excess uridine for 30 min where they progressed to metaphase. The cells were then treated (+Rosc 90 min) or not (Control) with roscovitine for 90 min in the presence of excess uridine. Cells appearing as early G1 cells were cultured with excess uridine for an additional 90 min after removal (+Rosc 90 min –Rosc 90 min) or without removal (+Rosc 180 min) of roscovitine. The cells were processed to reveal EU incorporation and to observe Nop52–GFP. Scale bar: 10 µm.

m-pre-rRNAs relocate in nucleoli at exit from mitosis

m-pre-rRNAs were still present, at least as 32S pre-rRNAs, in HeLa cells 2 h after release of the nocodazole block (Fig. 3C), and in colcemid-arrested mitotic HeLa cells treated for 2 or 6 h with CDK inhibitors (Fig. 4B,C; Fig. 5A,B) and they were detected in reformed nucleoli in indirubin-3′-monoxime-treated prometaphase cells (Fig. 6Bc). The localization of m-pre-rRNAs in reforming nucleoli at exit from mitosis was further investigated by using the fact that roscovitine treatment impairs formation of nucleoli in a reversible manner (Sirri et al., 2002). Metaphase-synchronized Nop52–GFP HeLa cells were untreated or treated with roscovitine for 90 min, i.e. when cells proceeded through M–G1 transition (Fig. 7, Control and +Rosc 90 min). Cells appearing as early G1 cells were cultured for an additional 90 min after removal (Fig. 7, +Rosc 90 min −Rosc 90 min) or without removal (Fig. 7, +Rosc 180 min) of roscovitine. It should be noted that for synchronization in metaphase, the cells were first accumulated at prometaphase by nocodazole treatment in the presence of EU to label m-pre-rRNAs. Prometaphase cells were then extensively washed and released into nocodazole-free medium containing a tenfold excess of uridine for 30 min where they proceeded to metaphase. Finally, metaphase cells were treated as specified above in the presence of excess uridine to minimize the incorporation of EU after resumption of rDNA transcription. As expected, independently of roscovitine treatment, the cells proceeded through mitosis and emerged after 90 min as early G1 cells (Fig. 7, Control and +Rosc 90 min). In control cells, Nop52 and EU-labeled pre-rRNAs mainly localized in the reformed nucleoli with a minor proportion still localized in PNBs. When reformation of nucleoli was prevented by roscovitine treatment, both Nop52 and EU-labeled pre-rRNAs were detected in the same small dots in the nucleus. After reversion of the effects of roscovitine on nucleologenesis (Fig. 7, +Rosc 90 min −Rosc 90 min), both Nop52 and EU-labeled pre-rRNAs localized in reformed nucleoli. When cells were maintained in roscovitine-containing culture medium (Fig. 7, +Rosc 180 min), both Nop52 and EU-labeled pre-rRNAs were still observed in the same small nuclear dots. Therefore, remarkably, EU-labeled pre-rRNAs were detected localized similarly to Nop52 in cells treated or not treated with roscovitine, i.e. in PNBs and reforming nucleoli.

However, even if the experiment was performed with excess uridine to minimize incorporation of EU after resumption of rDNA transcription, we could not be absolutely certain that nucleolar EU labeling was not the result of post-mitotic synthesis as rDNA transcription restarted in reforming nucleoli. To exclude this possibility, experimental conditions that render post-mitotic synthesis undetectable were first defined. Post-mitotic synthesis could be detected as FU or EU incorporation in reforming nucleoli of early G1 cells as shown in Fig. 8Aa,b by comparing the detection of FU- or EU-labeled RNAs and the nucleolar marker fibrillarin. For this, nocodazole-arrested prometaphase HeLa cells were maintained for 1 h in medium containing EU or FU (Fig. 8Ab, −Uridine). After this uptake step, the cells were washed and released for 2 h in nocodazole-free medium containing excess uridine. Conversely, post-mitotic synthesis was no longer detected when the uptake step was carried out in the presence of excess uridine in addition to EU or FU (Fig. 8Ab, +Uridine). Similar experiments were then performed except that the cells were synchronized in prometaphase in the presence of EU to also detect the pre-mitotically-labeled pre-rRNAs (Fig. 8Ba,b). The prometaphase cells were then washed and maintained for 1 h in medium containing FU alone (Fig. 8Bb, −Uridine) or FU together with excess uridine (Fig. 8Bb, +Uridine) before being washed and finally released for 2 h in nocodazole-free medium containing excess uridine where they progressed to early G1. When post-mitotic synthesis was detectable (Fig. 8Bb, −Uridine), EU and FU labeling mainly co-localized. When post-mitotic synthesis was no longer detectable (Fig. 8Bb, +Uridine), EU labeling, corresponding only to pre-mitotic synthesis, was clearly observed in reforming nucleoli and in PNBs of early G1 cells as demonstrated by the detection of fibrillarin. Consequently, m-pre-rRNAs synthesized before repression of rDNA transcription during prophase, actually localize in reforming nucleoli at the exit from mitosis.

DISCUSSION

So far, cell biology studies on m-pre-rRNAs, principally based on the fluorescence *in situ* hybridization (FISH) approach, have brought a wealth of information. However, the FISH approach has limitations, especially for RNAs such as rRNAs synthesized as precursors. Indeed, except for probes specifically hybridizing the 47S pre-rRNA, no probe highlights a single mature or pre-rRNA. Disappearance of FISH signals, which occurs as the processing events take place, does not allow tracking of the resulting mature or pre-rRNA. Moreover, it is impossible to know when pre-rRNAs were synthesized and therefore impossible to discriminate between m-pre-rRNAs transiting through mitosis and neosynthesized pre-

Journal of Cell Science (2016) 129, 1592-1604 doi:10.1242/jcs.180521

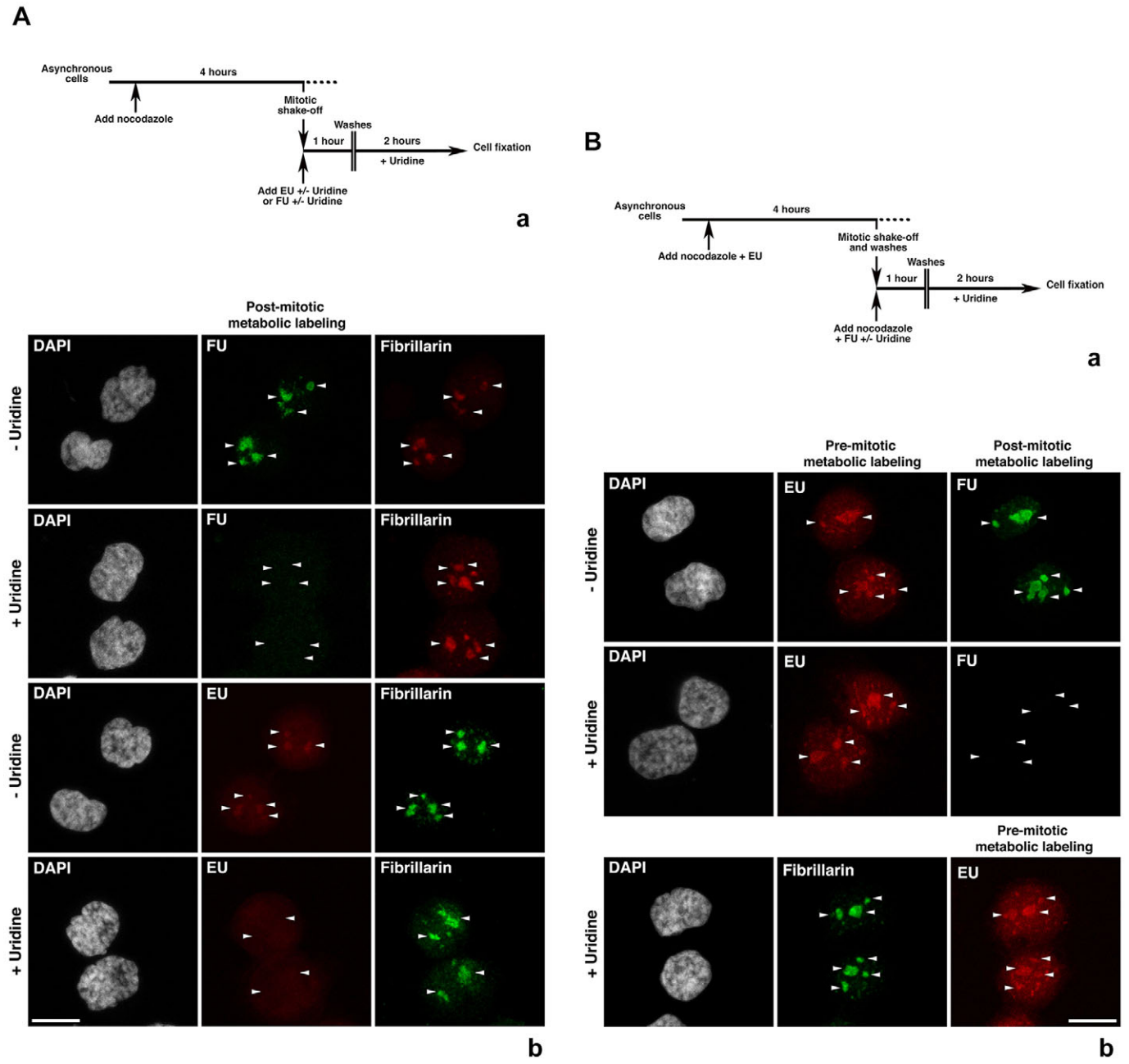

Fig. 8. m-pre-rRNAs relocate in nucleoli at M–G1 transition. (Aa) Schematic of the timing of the experiment. (Ab) Nocodazole-arrested prometaphase HeLa cells were resuspended in nocodazole-containing medium in the presence of EU or FU alone (−Uridine), or with excess uridine (+Uridine) for 1 h. The cells were then washed and cultured in nocodazole-free medium containing excess uridine for 2 h before being processed to observe fibrillarin and to reveal EU or FU post-mitotic incorporations. (Ba) Schematic of the timing of the experiment. (Bb) Nocodazole-arrested prometaphase HeLa cells accumulated in the presence of EU were washed and resuspended in nocodazole-containing medium in the presence of FU alone (−Uridine) or with excess uridine (+Uridine) for 1 h. The cells were then washed and cultured in nocodazole-free medium containing excess uridine for 2 h before being processed to detect EU pre-mitotic and FU post-mitotic incorporations, or to observe fibrillarin and reveal EU pre-mitotic incorporation. Arrowheads indicate the reforming nucleoli. Scale bars: 10 µm.

rRNAs. To overcome these limitations, we have globally followed metabolically labeled m-pre-rRNAs during and at exit from mitosis.

Pre-rRNA processing is transiently arrested during mitosis

Even if rDNA transcription is progressively repressed during prophase and restored at telophase, m-pre-rRNAs are maintained and transit through mitosis. We clearly observed that 45S, 32S and 30S pre-rRNAs remain associated with chromosomes. Other pre-rRNAs were not observed, showing that they are not maintained or maintained in very low amounts. These results agree with previous studies showing that 45S pre-rRNAs localize at the chromosome periphery in contrast to 47S and 46S pre-rRNAs (Carron et al., 2012). The arrest of pre-rRNA processing is supported by the presence of m-pre-rRNAs, especially the presence of the short-lived 45S pre-rRNA in HeLa cells blocked in mitosis for several hours. Because mitotic 45S pre-rRNA rapidly decreased in a manner unlikely related to degradation in colcemid-blocked mitotic HeLa cells after CDK inhibitor treatments, it may be proposed that as for rDNA transcription (Sirri et al., 2000), inhibition of pre-rRNA processing could be established at G2–M transition and/or

Journal of Cell Science (2016) 129, 1592-1604 doi:10.1242/jcs.180521

maintained during mitosis by a general CDK1–cyclin B-kinase-dependent mechanism. However, specific mechanisms might directly or indirectly inhibit specific steps of pre-rRNA processing. In particular, because 32S pre-rRNA processing depends on the presence of 5S rRNA (Dechampesme et al., 1999; Donati et al., 2013; Zhang et al., 2007), shutdown of 32S pre-rRNA processing might be linked to the regulation of Pol III transcription and/or any step involved in recruiting the RPL5–RPL11–5S rRNA precursor complex. In addition, as suggested by the presence of only 45S, 32S and 30S pre-rRNAs in mitotic cells (this study; Carron et al., 2012; Dundr and Olson, 1998), inhibition operates in a targeted manner on these pre-rRNA processing steps and logically excludes most pre-rRNA processing factors (Tafforeau et al., 2013) as potential targets.

Concerning the resumption of m-pre-rRNA processing, our results agree with the fact that maturation of m-pre-rRNAs is restored in PNBs at telophase (Carron et al., 2012) when CDK1–cyclin-B kinase is inhibited. However, as observed here, processing of mitotic 32S pre-rRNA occurs slowly and lasts during the M–G1 transition. Because the presence of 5S rRNA is required for 32S pre-rRNA processing (Dechampesme et al., 1999; Donati et al., 2013; Zhang et al., 2007) and as 5S RNP regulates the tumor suppressor p53 (Donati et al., 2013; Sloan et al., 2013), processing of mitotic 32S pre-rRNA could be correlated to cell-cycle progression.

m-pre-rRNAs determine the location of proteins at the chromosome periphery

Previous studies have shown that 45S pre-rRNA, in addition to small nucleolar RNAs and nucleolar proteins involved in the processing and modification of pre-rRNAs as well as in the assembly of mature rRNAs with ribosomal proteins, localize at the chromosome periphery during mitosis (Boisvert et al., 2007; Carron et al., 2012; DiMario, 2004; Dousset et al., 2000; Gautier et al., 1992; Hügle et al., 1985; Jiménez-García et al., 1994; Savino et al., 1999). Here, we show that 45S, 32S and 30S pre-rRNAs are maintained at the chromosome periphery and determine the location of pre-rRNA processing factors as demonstrated for fibrillarin, Nop58 and nucleolin. As pre-rRNP complexes were shown to be present in mitotic cells (Piñol-Roma, 1999), this observation indicates that m-pre-rRNAs are most probably the RNA moieties of pre-rRNP complexes present at the chromosome periphery. Beyond the presence of pre-rRNP complexes, the presence of pre-ribosomal particles is strongly suggested by the fact that processing of mitotic 45S pre-rRNAs is rapidly reactivated after CDK inhibitor treatments (this study) as is also the case of the Pol I transcription machinery (Sirri et al., 2000). Moreover, in addition to the effects on rDNA transcription and m-pre-rRNA processing, CDK inhibitor treatments induce the formation of PNBs (Sirri et al., 2002) where pre-ribosomal particles were visualized (Carron et al., 2012). The presence of 45S, 32S and 30S pre-rRNAs most probably indicates that 90S pre-ribosomal, pre-60S and pre-40S ribosomal particles are present at the chromosome periphery. As the location of proteins at the chromosome periphery is determined by m-pre-rRNAs and given the primary role of Ki-67 in establishing the perichromosomal compartment (Booth et al., 2014), Ki-67 is most probably implicated in localizing 90S pre-ribosomal, pre-60S and pre-40S ribosomal particles.

The function of the perichromosomal compartment remains unclear. However, in its absence, significant differences in nucleolar reassembly and nuclear organization were observed in post-mitotic cells (Booth et al., 2014). The involvement of components of the perichromosomal compartment such as nucleolin and RRS1 in the progression of mitosis, especially in chromosome congression, was also proposed (Gambe et al., 2009; Li et al., 2009; Ma et al., 2007).

Fate of mitotic pre-rRNPs at exit from mitosis

Whether or not postmitotic nucleoli are partly constructed from assembled components present in PNBs remains unknown (Dundr et al., 2000). However, a revised model was proposed in which PNBs would be autonomous extra-nucleolar ribosome maturation sites dedicated to processing of m-pre-rRNAs independently of processing of neosynthesized pre-rRNAs in the incipient nucleoli (Carron et al., 2012). The disassembly of PNBs would result from maturation and release of their pre-ribosome content and progressive release of processing factors. From loss-of-function experiments, the authors concluded that PNB disappearance depends on the processing of m-pre-rRNAs (Carron et al., 2012). However, such experiments alter processing of m-pre-rRNAs in PNBs and of neosynthesized pre-rRNAs in incipient nucleoli and, therefore, do not allow actual discrimination between direct and indirect effects. In agreement with the model, m-pre-rRNAs are processed in cells without functional nucleoli as in prometaphase cells treated with roscovitine, with AMD and roscovitine, or with AMD and indirubin-3′-monoxime. Nevertheless, processing of m-pre-rRNAs occurs without dissolution of PNBs in these cells. Conversely, dissolution of PNBs occurs as cells progress through M–G1 transition and in prometaphase cells treated with indirubin-3′-monoxime, i.e. in cells exhibiting functional nucleoli as assessed by rDNA transcription and processing of neosynthesized pre-rRNAs. Consequently, processing of m-pre-rRNAs is not sufficient to induce disappearance of PNBs that seems to require the presence of functional nucleoli.

Even though processing of m-pre-rRNAs can occur in PNBs, there is no evidence that m-pre-rRNAs are entirely processed in PNBs and exported to the cytoplasm. Conversely, we observed the presence of rRNAs that originate from m-pre-rRNAs in reforming nucleoli at the M–G1 transition. In addition, processing of m-pre-rRNAs exhibits a marked difference in timing between pre-40S and pre-60S ribosomal particles (this study; Carron et al., 2012; Dundr et al., 2000); especially, the duration of 32S pre-rRNA processing, which is so long that it could appear somewhat difficult to reconcile with the lifetime of PNBs.

Even though further experiments are needed to uncover their roles, it is tempting to propose that mitotic pre-rRNPs might be involved in reforming functional nucleoli. This hypothesis is corroborated by results obtained using CDK inhibitors. Indeed, the CDK inhibitor roscovitine impairs relocalization of mitotic pre-rRNPs from PNBs to the sites of resumption of rDNA transcription as assessed by the pre-rRNA processing factor Nop52 (Yoshikawa et al., 2015) and the m-pre-rRNAs, and prevents formation of functional nucleoli as evidenced by the processing defect of neosynthesized pre-rRNAs. Conversely, the CDK inhibitor indirubin-3′-monoxime impairs neither relocalization of mitotic pre-rRNPs nor formation of functional nucleoli, suggesting that both events are related. Moreover, the nucleolar localization of the 40S and/or 60S ribosomal subunit precursors generated from the mitotic pre-rRNPs might be a prerequisite for their export.

Like the disappearance of PNBs that requires the presence of functional nucleoli, nucleolar localization of m-pre-rRNAs reflects the close relationship between PNBs and nucleoli. Given that the 5S RNP can regulate the tumor suppressor p53 (Donati et al., 2013; Sloan et al., 2013) and that it plays a crucial role in 32S pre-rRNA processing (Dechampesme et al., 1999; Donati et al., 2013; Zhang et al., 2007), the processing of m-pre-rRNAs, disappearance of

Journal of Cell Science (2016) 129, 1592-1604 doi:10.1242/jcs.180521

PNBs, M–G1 progression and the formation of functional nucleoli are very likely correlated. Thus once formed, nucleoli can regulate cell cycle progression (Tsai and Pederson, 2014).

MATERIALS AND METHODS

Antibodies

The human autoimmune serum with specificity against fibrillarin (O61; 1:3000) was described previously (Sirri et al., 2002). The anti-fibrillarin [anti-FBL (126-140); 1:10,000], anti-BrdU (clone BU-33; 1:500), anti-UBF (clone 6B6; 1:10,000) antibodies were from Sigma-Aldrich. The anti-nucleolin (MS-3; 1:1000) and anti-Nop58 (C-20; 1:1000) antibodies were from Santa Cruz Biotechnology. The alkaline phosphatase-conjugated anti-digoxigenin antibodies were from Roche (11 093 274 910; 1:20,000). The secondary antibodies coupled to Alexa Fluor 488 (109-545-088 and 115-545-166; 1:500), Alexa Fluor 594 (109-585-088; 1:500) and Alexa Fluor 647 (709-605-149; 1:500) were from Jackson ImmunoResearch Laboratories, Inc. and those coupled to horseradish peroxidase were from Sigma-Aldrich (A5420; 1:10,000) and Jackson ImmunoResearch Laboratories (111-035-003 and 115-035-003; 1:3000).

Primers

PCRs and/or real-time PCRs were performed using oligonucleotides corresponding to human rDNA (see Fig. S1). The forward oligonucleotides were ETS1: 5′-GAGGTTGGGCCTCCGGATGC-3′, ETS3: 5′-CCTCTGACGCGGCAGACAGC-3′, ETS5: 5′-GTCGGTGT-GGGGTTCGAGGC-3′, 5.8S1: 5′-CACTTCGAACGCACTTGCGG-3′ and 18S1: 5′-GTTCAAAGCAGGCCCGAGCC-3′, and the reverse oligonucleotides were ETS2: 5′-ACGCGCGAGAGAACAGCAGG-3′, ETS4: 5′-CTCCAGGAGCACCGCAAGGG-3′, ETS6: 5′-CCACCGC-GATCGCTCACACG-3′, 5.8S2: 5′-CTGCGAGGGAACCCCCAGCC-3′ and 18S2: 5′-AGCGGCGCAATACGAATGCC-3′.

Probes

The ETS (nt +935/+1082), 18S (nt +4477/+4610) and 5.8S+ (nt +6718/+6845) probes corresponding to human rDNA were generated as digoxigenin-labeled using primers ETS5 and ETS6, primers 18S1 and 18S2, and primers 5.8S1 and 5.8S2, respectively, and the PCR DIG probe synthesis kit (Roche).

Cell culture and synchronization, inhibitor treatments and siRNA transfections

Stably transfected Nop52–GFP (Savino et al., 2001) and untransfected HeLa cell lines were cultured in MEM supplemented with 10% FCS and 2 mM L-glutamine (GIBCO BRL). The cells blocked in prometaphase by nocodazole (0.04 µg/ml, Sigma-Aldrich) or colcemid (KaryoMax colcemid solution at 0.02 µg/ml, GIBCO BRL) treatments for 4 h or overnight were selectively harvested by mechanical shock. For metaphase synchronization, the cells were arrested in prometaphase by nocodazole treatment for 4 h, washed and resuspended in nocodazole-free medium for 30 min. For chromosome preparations, the cells were blocked in prometaphase by colcemid treatment for 4 h in the presence or absence of AMD (0.05 µg/ml, Sigma-Aldrich) added 1 h before the colcemid solution. For immunofluorescence and *in situ* transcription assays, asynchronous cells were grown as monolayers on glass slides, and synchronized mitotic cells were transferred onto poly-L-lysine-coated glass slides.

The cells were treated with AMD (0.05 µg/ml) to specifically inhibit rDNA transcription and with the CDK inhibitors roscovitine (75 µM) or indirubin-3′-monoxime (25 µM) obtained from Sigma-Aldrich.

The cells were transfected with the siControl RISC-free siRNA (Dharmacon) and the nucleolin targeting siRNA (SI02654925, Qiagen) using INTERFERin™ (Polyplus-transfection) the day of cell seeding and grown for 48 h before the experiments.

RNA metabolic labeling

To analyze the timing of synthesis of m-pre-rRNAs, asynchronous cells were cultured in medium containing 100 µM EU for 3 h to which 1 mM FU was added for the last 30 or 60 min of culture. To analyze the fate of m-pre-rRNAs, prometaphase cells were collected in the presence of 100 µM EU, extensively washed and resuspended in EU-free medium or in EU-free medium containing uridine (1 mM). To evaluate the influence of post-mitotic RNA synthesis on EU labeling observed after mitosis, the cells were accumulated by nocodazole treatment, selectively harvested and resuspended in nocodazole-containing medium in the presence of 100 µM EU or 10 µM FU alone or with 1 mM uridine, extensively washed before being resuspended in nocodazole-free medium containing 1 mM uridine. To determine the influence of nucleolin on rRNA synthesis, HeLa cells treated with siRNAs were cultured in medium containing 1 mM FU for the last 1 h.

In situ detection of rDNA transcription, of FU- and/or EU-labeled RNAs and immunofluorescence labeling

rDNA transcription was detected in fixed cells as previously described (Roussel et al., 1996) and BrUTP incorporation was detected using anti-BrdU antibodies revealed by the Alexa-Fluor-488- or 594-conjugated anti-mouse antibodies. For the detection of FU-labeled RNAs and/or EU-labeled RNAs and/or fibrillarin, the cells were fixed with methanol for 20 min at −20°C, air-dried for 5 min and rehydrated with PBS for 5 min. FU incorporation was detected similarly to BrUTP incorporation. EU incorporation was detected using the Click-iT RNA Imaging kit (Invitrogen) introducing the Alexa Fluor 594 dye. Fibrillarin was detected using the O61 serum revealed by Alexa-Fluor-647-conjugated anti-human antibodies. When EU-labeled RNAs were to be detected simultaneously with BrUTP incorporation, FU-labeled RNAs or fibrillarin, the cells were post-fixed in 4% paraformaldehyde for 15 min at room temperature after the incubations of antibodies before EU detection. All preparations were mounted with the Fluoroshield antifading solution containing 4,6-diamidino-2-phenylindole (DAPI, Sigma-Aldrich). The cells were imaged by fluorescence microscopy performed using a Leica upright SP5 confocal microscope with a 63× objective and version 2.7.3 of the Leica Application Suite Advanced Fluorescence software. Multiple fluorophores were recorded sequentially at each *z*-step. Projections of *z*-series and merge images were performed using ImageJ software (NIH).

Chromosome preparation

The procedure used to isolate chromosomes was adapted from Paulson (1982). The solutions contained RNaseOUT™ recombinant ribonuclease inhibitor (Invitrogen) and Protease Inhibitor Cocktail (Sigma-Aldrich). For each preparation, about 2×10^7 prometaphase cells were pelleted at 100 ***g*** for 10 min, suspended in 10 ml 0.5× buffer A (15 mM Tris-HCl pH 7.4, 0.2 mM spermine, 0.5 mM spermidine, 2 mM EDTA and 80 mM KCl) and incubated at room temperature for 10 min. Swollen cells were collected by centrifugation at 4°C (200 ***g*** for 15 min) and resuspended in 5 ml 1× chilled buffer A containing 0.1% NP40. All subsequent steps were carried out at 4°C. Cells were then disrupted by passage through a G26 needle. To discard contaminating cells and nuclei, the chromosome suspension was centrifuged on a 0.25 M sucrose cushion in buffer A containing 0.1% NP40 at 250 ***g*** for 5 min, and the supernatant re-centrifuged on a 0.5 M sucrose cushion in buffer A containing 0.1% NP40 at 2000 ***g*** for 20 min. The purity of the chromosome pellet was verified by fluorescence microscopy after DAPI staining and the pellet resuspended in SDS-PAGE sample buffer for protein analysis or in NucleoSpin RNA lysis buffer (Macherey-Nagel) for RNA analysis.

Immunoblotting

Protein extracts were prepared by resuspending pellets containing whole mitotic cells or purified chromosomes in SDS-PAGE sample buffer, sonicated, boiled for 5 min and centrifuged. Whole mitotic cell (20 µg) and purified chromosome (10 µg) protein extracts were resolved by SDS-PAGE, transferred to nitrocellulose membranes (Protran, Schleicher and Schuell). The membranes were incubated with anti-UBF, anti-nucleolin, anti-Nop58 or anti-fibrillarin antibodies revealed by suitable horseradish peroxidase-conjugated secondary antibodies and immunoreactivity detected by chemiluminescence (GE Healthcare).

RNA analysis

RNAs were extracted from cells and from purified chromosomes using NucleoSpin RNA and separated (4 µg for cells and 400 ng for

chromosomes) in 0.8% agarose formaldehyde gels. For northern blot analyses, RNAs were transferred to positively charged membranes (Roche). Hybridization was carried out using DIG Easy Hyb buffer (Roche) at 50°C. After washes, the probe was revealed using the DIG Wash and Block Buffer Set (Roche) and the alkaline-phosphatase-conjugated anti-digoxigenin antibodies. Alkaline phosphatase activity was detected using the chemiluminescent substrate CDP-Star (Roche) and quantified with the ImageJ software.

RT-qPCR

Total RNA was quantified, electrophoresed to verify its quality and reverse-transcribed (2 µg) with the Superscript First-Strand Synthesis System for RT-PCR (Invitrogen) using random hexamers as primers (125 ng). Real-time PCR was performed using LightCycler 480 SYBR Green I Master and run on a LightCycler 480 II device (Roche). For each reaction, 1.5% synthesized cDNA and 1 µM of a pair of specific primers, either ETS1 and ETS2, ETS3 and ETS4, or 5.8S1 and 5.8S2, were used. Normalization was performed using primers 18S1 and 18S2, which primarily amplify the cDNAs corresponding to mature 18S rRNA. Amplification efficiency for each assay was determined by running a standard dilution curve. Cycle threshold values and relative quantifications were calculated by the LightCycler 480 software.

Acknowledgements

The authors thank the imaging and real-time PCR platforms of the Institut de Biologie Paris Seine and A.L. Haenni for critical reading of the manuscript.

Competing interests

The authors declare no competing or financial interests.

Author contributions

V.S. designed, performed and analyzed the experiments. N.J. performed all analyses by confocal microscopy. P.R. supervised the project, designed, performed and analyzed the experiments, and co-wrote the manuscript with D.H.-V.

Funding

This study was supported in part by grants from the Centre National de la Recherche Scientifique, the UPMC Université Paris 06 and the Université Paris Diderot.

Supplementary information

Supplementary information available online at
http://jcs.biologists.org/lookup/suppl/doi:10.1242/jcs.180521/-/DC1

References

Boisvert, F.-M., van Koningsbruggen, S., Navascués, J. and Lamond, A. I. (2007). The multifunctional nucleolus. *Nat. Rev. Mol. Cell Biol.* **8**, 574-585.

Booth, D. G., Takagi, M., Sanchez-Pulido, L., Petfalski, E., Vargiu, G., Samejima, K., Imamoto, N., Ponting, C. P., Tollervey, D., Earnshaw, W. C. et al. (2014). Ki-67 is a PP1-interacting protein that organises the mitotic chromosome periphery. *eLife* **3**, e01641.

Carron, C., Balor, S., Delavoie, F., Plisson-Chastang, C., Faubladier, M., Gleizes, P.-E. and O'Donohue, M.-F. (2012). Post-mitotic dynamics of pre-nucleolar bodies is driven by pre-rRNA processing. *J. Cell Sci.* **125**, 4532-4542.

Chen, Q., Zhang, X., Jiang, Q., Clarke, P. R. and Zhang, C. (2008). Cyclin B1 is localized to unattached kinetochores and contributes to efficient microtubule attachment and proper chromosome alignment during mitosis. *Cell Res.* **18**, 268-280.

Dechampesme, A.-M., Koroleva, O., Leger-Silvestre, I., Gas, N. and Camier, S. (1999). Assembly of 5S ribosomal RNA is required at a specific step of the pre-rRNA processing pathway. *J. Cell Biol.* **145**, 1369-1380.

DiMario, P. J. (2004). Cell and molecular biology of nucleolar assembly and disassembly. *Int. Rev. Cytol.* **239**, 99-178.

Donati, G., Peddigari, S., Mercer, C. A. and Thomas, G. (2013). 5S ribosomal RNA is an essential component of a nascent ribosomal precursor complex that regulates the Hdm2-p53 checkpoint. *Cell Rep.* **4**, 87-98.

Dousset, T., Wang, C., Verheggen, C., Chen, D., Hernandez-Verdun, D. and Huang, S. (2000). Initiation of nucleolar assembly is independent of RNA polymerase I transcription. *Mol. Biol. Cell* **11**, 2705-2717.

Dundr, M. and Olson, M. O. J. (1998). Partially processed pre-rRNA is preserved in association with processing components in nucleolus-derived foci during mitosis. *Mol. Biol. Cell* **9**, 2407-2422.

Dundr, M., Misteli, T. and Olson, M. O. J. (2000). The dynamics of postmitotic reassembly of the nucleolus. *J. Cell Biol.* **150**, 433-446.

Fan, H. and Penman, S. (1971). Regulation of synthesis and processing of nucleolar components in metaphase-arrested cells. *J. Mol. Biol.* **59**, 27-42.

Gambe, A. E., Matsunaga, S., Takata, H., Ono-Maniwa, R., Baba, A., Uchiyama, S. and Fukui, K. (2009). A nucleolar protein RRS1 contributes to chromosome congression. *FEBS Lett.* **583**, 1951-1956.

Gassmann, R., Henzing, A. J. and Earnshaw, W. C. (2005). Novel components of human mitotic chromosomes identified by proteomic analysis of the chromosome scaffold fraction. *Chromosoma* **113**, 385-397.

Gautier, T., Robert-Nicoud, M., Guilly, M. N. and Hernandez-Verdun, D. (1992). Relocation of nucleolar proteins around chromosomes at mitosis. A study by confocal laser scanning microscopy. *J. Cell Sci.* **102**, 729-737.

Henras, A. K., Soudet, J., Gérus, M., Lebaron, S., Caizergues-Ferrer, M., Mougin, A. and Henry, Y. (2008). The post-transcriptional steps of eukaryotic ribosome biogenesis. *Cell. Mol. Life Sci.* **65**, 2334-2359.

Hügle, B., Hazan, R., Scheer, U. and Franke, W. W. (1985). Localization of ribosomal protein S1 in the granular component of the interphase nucleolus and its distribution during mitosis. *J. Cell Biol.* **100**, 873-886.

Jiménez-García, L. F., Segura-Valdez, M. L., Ochs, R. L., Rothblum, L. I., Hannan, R. and Spector, D. L. (1994). Nucleologenesis: U3 snRNA-containing prenucleolar bodies move to sites of active pre-rRNA transcription after mitosis. *Mol. Biol. Cell* **5**, 955-966.

Li, N., Yuan, K., Yan, F., Huo, Y., Zhu, T., Liu, X., Guo, Z. and Yao, X. (2009). PinX1 is recruited to the mitotic chromosome periphery by Nucleolin and facilitates chromosome congression. *Biochem. Biophys. Res. Commun.* **384**, 76-81.

Ma, N., Matsunaga, S., Takata, H., Ono-Maniwa, R., Uchiyama, S. and Fukui, K. (2007). Nucleolin functions in nucleolus formation and chromosome congression. *J. Cell Sci.* **120**, 2091-2105.

Mullineux, S.-T. and Lafontaine, D. L. J. (2012). Mapping the cleavage sites on mammalian pre-rRNAs: Where do we stand? *Biochimie* **94**, 1521-1532.

Muro, E., Gébrane-Younès, J., Jobart-Malfait, A., Louvet, E., Roussel, P. and Hernandez-Verdun, D. (2010). The traffic of proteins between nucleolar organizer regions and prenucleolar bodies governs the assembly of the nucleolus at exit of mitosis. *Nucleus* **1**, 202-211.

Ohta, S., Bukowski-Wills, J.-C., Sanchez-Pulido, L., Alves, F. d. L., Wood, L., Chen, Z. A., Platani, M., Fischer, L., Hudson, D. F., Ponting, C. P. et al. (2010). The protein composition of mitotic chromosomes determined using multiclassifier combinatorial proteomics. *Cell* **142**, 810-821.

Paulson, J. R. (1982). Isolation of chromosome clusters from metaphase-arrested HeLa cells. *Chromosoma* **85**, 571-581.

Phillips, S. G. (1972). Repopulation of the postmitotic nucleolus by preformed RNA. *J. Cell Biol.* **53**, 611-623.

Piñol-Roma, S. (1999). Association of nonribosomal nucleolar proteins in ribonucleoprotein complexes during interphase and mitosis. *Mol. Biol. Cell* **10**, 77-90.

Popov, A., Smirnov, E., Kováčik, L., Raška, O., Hagen, G., Stixová, L. and Raška, I. (2013). Duration of the first steps of the human rRNA processing. *Nucleus* **4**, 134-141.

Roussel, P., André, C., Comai, L. and Hernandez-Verdun, D. (1996). The rDNA transcription machinery is assembled during mitosis in active NORs and absent in inactive NORs. *J. Cell Biol.* **133**, 235-246.

Savino, T. M., Bastos, R., Jansen, E. and Hernandez-Verdun, D. (1999). The nucleolar antigen Nop52, the human homologue of the yeast ribosomal RNA processing RRP1, is recruited at late stages of nucleologenesis. *J. Cell Sci.* **112**, 1889-1900.

Savino, T. M., Gébrane-Younès, J., De Mey, J., Sibarita, J.-B. and Hernandez-Verdun, D. (2001). Nucleolar assembly of the rRNA processing machinery in living cells. *J. Cell Biol.* **153**, 1097-1110.

Sirri, V., Roussel, P. and Hernandez-Verdun, D. (2000). In vivo release of mitotic silencing of ribosomal gene transcription does not give rise to precursor ribosomal RNA processing. *J. Cell Biol.* **148**, 259-270.

Sirri, V., Hernandez-Verdun, D. and Roussel, P. (2002). Cyclin-dependent kinases govern formation and maintenance of the nucleolus. *J. Cell Biol.* **156**, 969-981.

Sloan, K. E., Bohnsack, M. T. and Watkins, N. J. (2013). The 5S RNP couples p53 homeostasis to ribosome biogenesis and nucleolar stress. *Cell Rep.* **5**, 237-247.

Tafforeau, L., Zorbas, C., Langhendries, J.-L., Mullineux, S.-T., Stamatopoulou, V., Mullier, R., Wacheul, L. and Lafontaine, D. L. J. (2013). The complexity of human ribosome biogenesis revealed by systematic nucleolar screening of pre-rRNA processing factors. *Mol. Cell* **51**, 539-551.

Toyoda, Y. and Yanagida, M. (2006). Coordinated requirements of human topo II and cohesin for metaphase centromere alignment under Mad2-dependent spindle checkpoint surveillance. *Mol. Biol. Cell* **17**, 2287-2302.

Tsai, R. Y. L. and Pederson, T. (2014). Connecting the nucleolus to the cell cycle and human disease. *FASEB J.* **28**, 3290-3296.

Westendorf, J. M., Konstantinov, K. N., Wormsley, S., Shu, M.-D., Matsumoto-Taniura, N., Pirollet, F., Klier, F. G., Gerace, L. and Baserga, S. J. (1998). M phase phosphoprotein 10 is a human U3 small nucleolar ribonucleoprotein component. *Mol. Biol. Cell* **9**, 437-449.

Wilkinson, D. S., Tlsty, T. D. and Hanas, R. J. (1975). The inhibition of ribosomal RNA synthesis and maturation in Novikoff hepatoma cells by 5-fluorouridine. *Cancer Res.* **35**, 3014-3020.

Yoshikawa, H., Ishikawa, H., Izumikawa, K., Miura, Y., Hayano, T., Isobe, T., Simpson, R. J. and Takahashi, N. (2015). Human nucleolar protein Nop52 (RRP1/NNP-1) is involved in site 2 cleavage in internal transcribed spacer 1 of pre-rRNAs at early stages of ribosome biogenesis. *Nucleic Acids Res.* **43**, 5524-5536.

Zhang, J., Harnpicharnchai, P., Jakovljevic, J., Tang, L., Guo, Y., Oeffinger, M., Rout, M. P., Hiley, S. L., Hughes, T. and Woolford, J. L. (2007). Assembly factors Rpf2 and Rrs1 recruit 5S rRNA and ribosomal proteins rpL5 and rpL11 into nascent ribosomes. *Genes Dev.* **21**, 2580-2592.

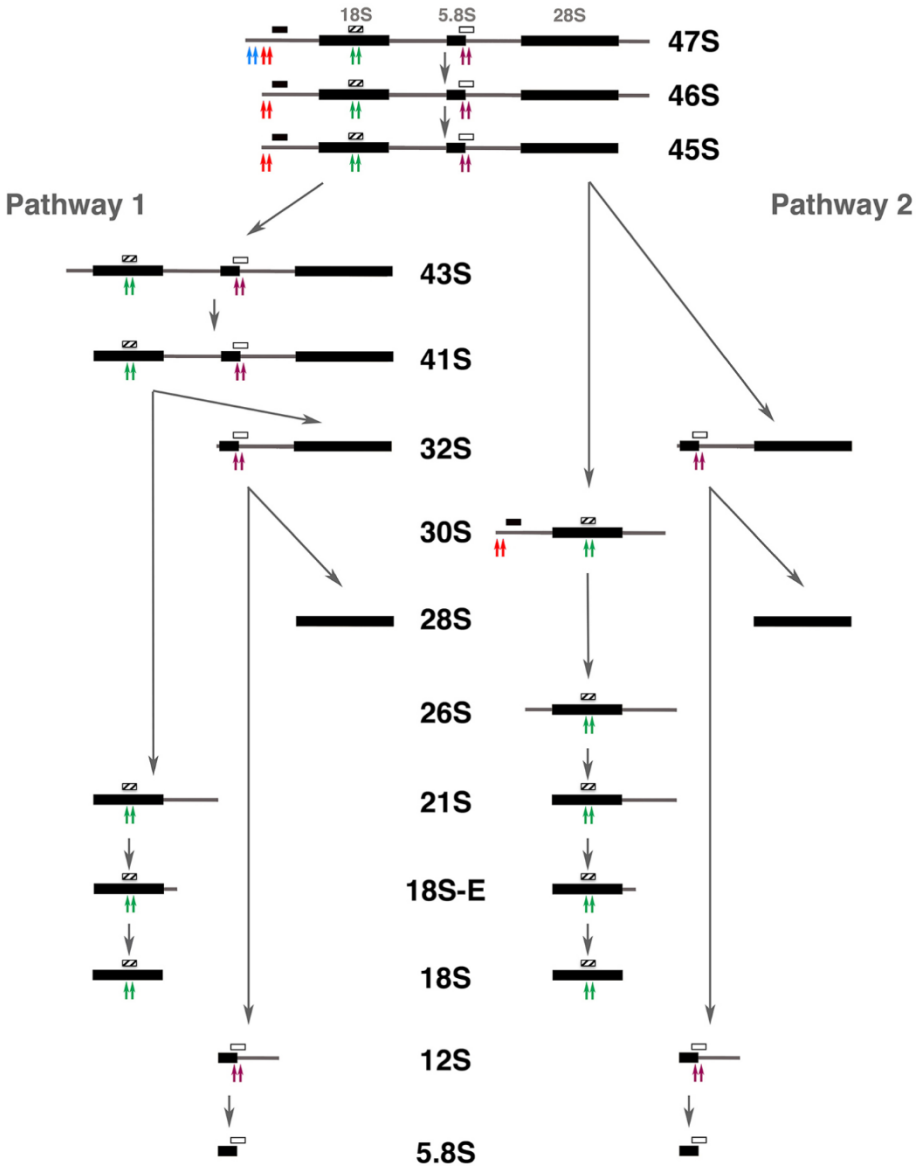

Fig. S1. Scheme of the two pre-rRNA processing pathways in human cells. Pre-rRNA processing involves numerous cleavages (arrows) following two alternative pathways. The primers used for RTqPCR experiments are indicated as double arrows in blue (ETS1, ETS2), red (ETS3, ETS4), green (18S1, 18S2) and purple (5.8S1, 5.8S2) as well as the ETS (closed rectangle), 18S (hatched rectangle) and 5.8S+ (open rectangle) probes used for northern blots (open rectangle).

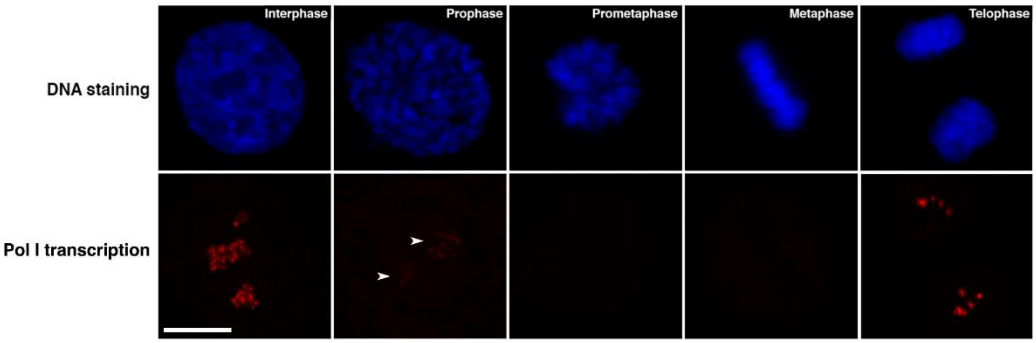

Fig. S2. Pol I transcription is progressively repressed during prophase and restored in telophase. HeLa cells were observed at different stages of the cell cycle identified by DNA staining. The *in situ* detection of Pol I transcription revealed that transcription is progressively repressed in prophase (arrowheads) and maintained repressed during mitosis until telophase when Pol I transcription was restored. Bar, 10 μm.

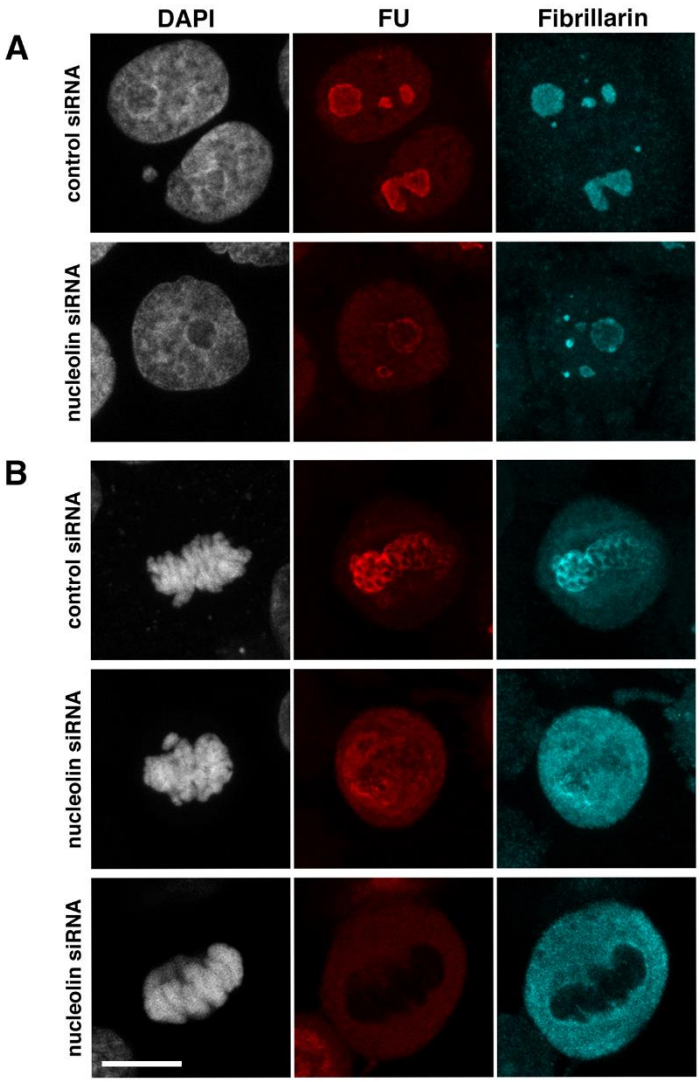

Fig. S3. m-Pre-rRNAs determine the location of fibrillarin at the chromosome periphery. Hela cells treated with a control siRNA or a nucleolin targeting siRNA were cultured in FU- (1 mM) containing medium for 1 h. The FU-labeled RNAs and fibrillarin were analyzed in interphase (A) and metaphase (B) cells. Bar, 10 μm.

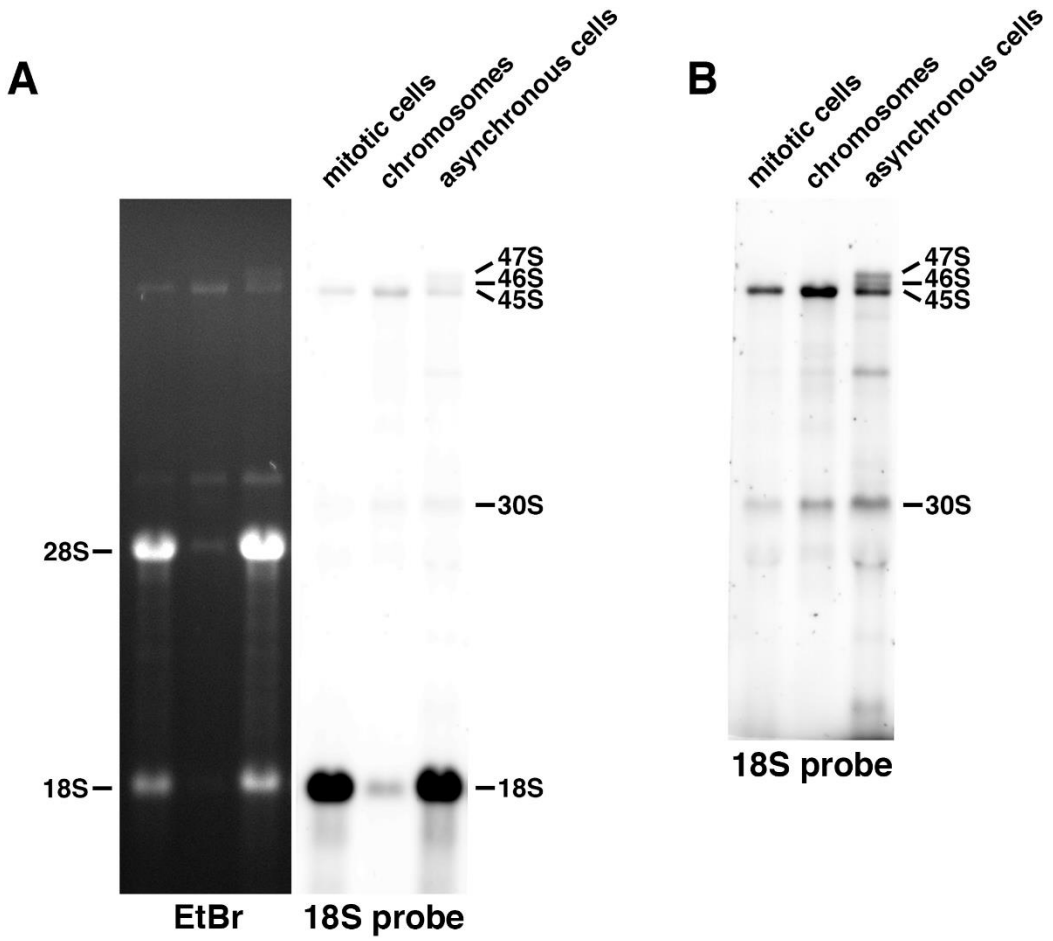

Fig. S4. Identification of m-pre-rRNAs associated with chromosomes. (A, B) RNAs were isolated from colcemid-blocked prometaphase HeLa cells (mitotic cells), from purified chromosomes (chromosomes) and from asynchronous Hela cells (asynchronous cells). After separation in a gel (EtBr), RNAs were blotted and hybridized with the 18S probe (18S probe). (A) The hybridized probe was revealed for a short exposure time. (B) The probe hybridized on the upper part of the blot was revealed for a long exposure time.